Size distribution and chemical composition of secondary organic aerosol formed from Cl-initiated oxidation of toluene

Mingqiang Huang[1,2,3], Weijun Zhang[1,2,*], Xuejun Gu[1,2], Changjin Hu[1,2],
Weixiong Zhao[1,2], Zhenya Wang[1,2], Li Fang[1,2]

1. Key Laboratory of Atmospheric Composition and Optical Radiation, Anhui Institute of Optics & Fine Mechanics, Chinese Academy of Sciences, Hefei 230031, China. E-mail: huangmingqiang@gmail.com
2. Laboratory of Environment Spectroscopy, Anhui Institute of Optics & Fine Mechanics, Chinese Academy of Sciences, Hefei 230031, China
3. Department of Environmental Science and Engineering, Xiamen University, Tan Kah Kee College, Zhangzhou 363105, China

Abstract

Secondary organic aerosol (SOA) formed from Cl-initiated oxidation of toluene was investigated in a home-made smog chamber. The size distribution and chemical composition of SOA particles were measured using aerodynamic particle sizer spectrometer and the aerosol laser time-of-flight mass spectrometer (ALTOFMS), respectively. According to a large number of single aerosol diameter and mass spectra, the size distribution and chemical composition of SOA were obtained statistically. Experimental results showed that SOA particles created by Cl-initiated oxidation of toluene is predominantly in the form of fine particles, which have diameters less than 2.5 μm (i.e., PM2.5), and glyoxal, benzaldehyde, benzyl alcohol, benzoquinone, benzoic acid, benzyl hydroperoxide and benzyl methyl nitrate are the major products components in the SOA. The possible reaction mechanisms leading to these products are also proposed.

Key words: toluene; Cl-initiated oxidation; secondary organic aerosol; smog chamber, laser desorption/ionization

DOI: 10.1016/S1001-0742(11)60840-1

Introduction

Aromatic compounds such as benzene, toluene, and xylene include a significant portion of the volatile organic compounds (VOC) in urban areas, and toluene is the most abundant aromatic hydrocarbon among them (Odum et al., 1997; Jang and Kamens, 2001). In the troposphere, toluene can be transformed by gas-phase reactions with hydroxyl (OH) radicals, nitrate (NO$_3$) radicals, ozone (O$_3$), and, possibly, chlorine (Cl) atoms (Atkinson and Arey, 2003). Although reactions with OH radicals, NO$_3$ radicals, and O$_3$ are generally considered to be the major transformation processes of toluene, the importance of Cl atom reactions in the Arctic lower troposphere during springtime has become apparent (Ramacher et al., 1997; Ariya et al., 1999). It has been postulated that Cl atom reactions may also be significant in the marine boundary layer and in coastal regions (Oum et al., 1998; Spicer et al., 1998; Kercher et al., 2009).

Many estimates of tropospheric Cl atom concentrations have been made to evaluate the importance of Cl atom reactions as a loss process for certain VOC in the troposphere. Wingenter and co-workers (1999) derived OH radical and Cl atom concentrations in the marine boundary layers of $(2.6\pm0.7)\times10^6$ molecule/cm^3 and $(6.5\pm1.4)\times10^4$

molecule/cm^3, respectively. Concentration of Cl$_2$ of up to 150 ppt and of photolyzable chlorine up to 250 ppt have been reported in the marine boundary layer at dawn (Spicer et al., 1998). Photolysis of these species is expected to result in peak Cl atom concentration as high as or more in the marine boundary layer at dawn (Spicer et al., 1998). Because many organic compounds have rate constants for reaction with Cl atoms that are about 10^2 higher than those for reaction with OH radicals (Fantechi et al., 1998; Notario et al., 2000; Thiault et al., 2002), these ambient data indicate that Cl atoms reactions in the marine boundary layer, and perhaps also in coastal areas, could be significant.

Although there have been several studies of the reactions of Cl atoms with various classes of VOC, only a few studies of the reactions of Cl atoms with toluene have been performed to date (Shi and Bernhard, 1997; Karlsson et al., 2001; Wang et al., 2005; Cai et al., 2008). However, these studies often used off-line techniques, like GC/MS and CI-GC-ITMS system for products measurement; it is difficult to measure the size and chemical composition of individual secondary organic aerosol (SOA) particles simultaneously. Our laboratory has demonstrated that the aerosol laser time-of-flight mass spectrometer (ALTOFMS) can be used to measure the size and chemical composition of ethylbenzene SOA particles in real-time (Huang et al., 2010). In this

* Corresponding author. E-mail: wjzhang@aiofm.ac.cn

work, the oxidation of toluene was initiated by Cl atoms in a home-made smog chamber, aerodynamic particle sizer spectrometer TSI 3321 and ALTOFMS were employed to detect the individual particles in real-time.

1 Experimental method

Toluene (> 99%) was obtained from Sigma-Aldrich Chemistry Corporation, Germany. Cl_2 (99.9%) and nitrogen oxide (99.9%) was from Nanjing Special Gas Factory, China. All those chemicals were used without further purification.

Oxidation of toluene was performed using UV-irradiation of toluene/Cl_2/NO/ air mixtures in an 850-L sealed collapsible polyethylene smog chamber (Hao et al., 2007). Prior to the start of experiment, the chamber was continuously flushed with purified laboratory compressed air for 40 min. Toluene was sampled by a micro liter injector and directly transferred into the chamber. Cl_2 and NO were expanded into the evacuated manifold to reach the desired pressure level through Teflon lines, and then were introduced into the smog chamber by a stream of purified air. And again the chamber was filled with the purified air to 850 L full volume, then turn on four black lamps and initiate the photooxidation reaction. Cl atoms will be generated by the photolysis of Cl_2 in air at wavelengths longer than 300 nm (Atkinson and Aschmann, 1985). In all the experiments, the relative humidity was in the range of 65%–70%, and temperature was 295±2 K, the concentrations of toluene, NO, and Cl_2 were 2.0, 2.0, and 4.0 ppmV respectively. After one hour photooxidation, the size distribution and the chemical composition of SOA particles were detected by a TSI 3321 aerodynamic particle size spectrometer (TSI, model 3321, USA) and ALTOFMS

connected directly to the chamber using a Teflon line.

2 Results and discussion

2.1 Size distribution of the SOA particles

Figures 1 and 2 show the size distribution and particle number concentration of the SOA particles during the experiment of Cl-initiated oxidation of toluene. In the first 10 min of the reaction time, only few particle whose diameter less than 0.5 μm were detected by TSI 3321. As we all known, secondary organic aerosols are formed by reaction of Cl atoms with toluene to produce both semivolatile and nonvolatile products. And the gas-phase products begin to homogeneously nucleate only after a product exceeds of its saturation concentration (Odum et al., 1996; Bowman et al., 1997). Thus, until sufficient toluene has reacted to produce gas-phase concentrations that exceed
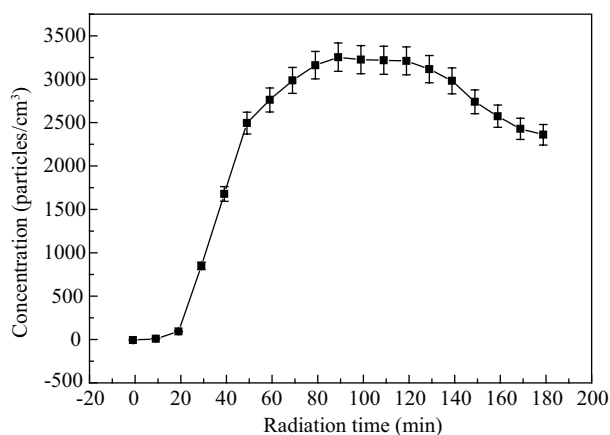
Fig. 2 Particle number concentration of SOA particles formed from Cl-initiated oxidation of toluene at different reaction time.
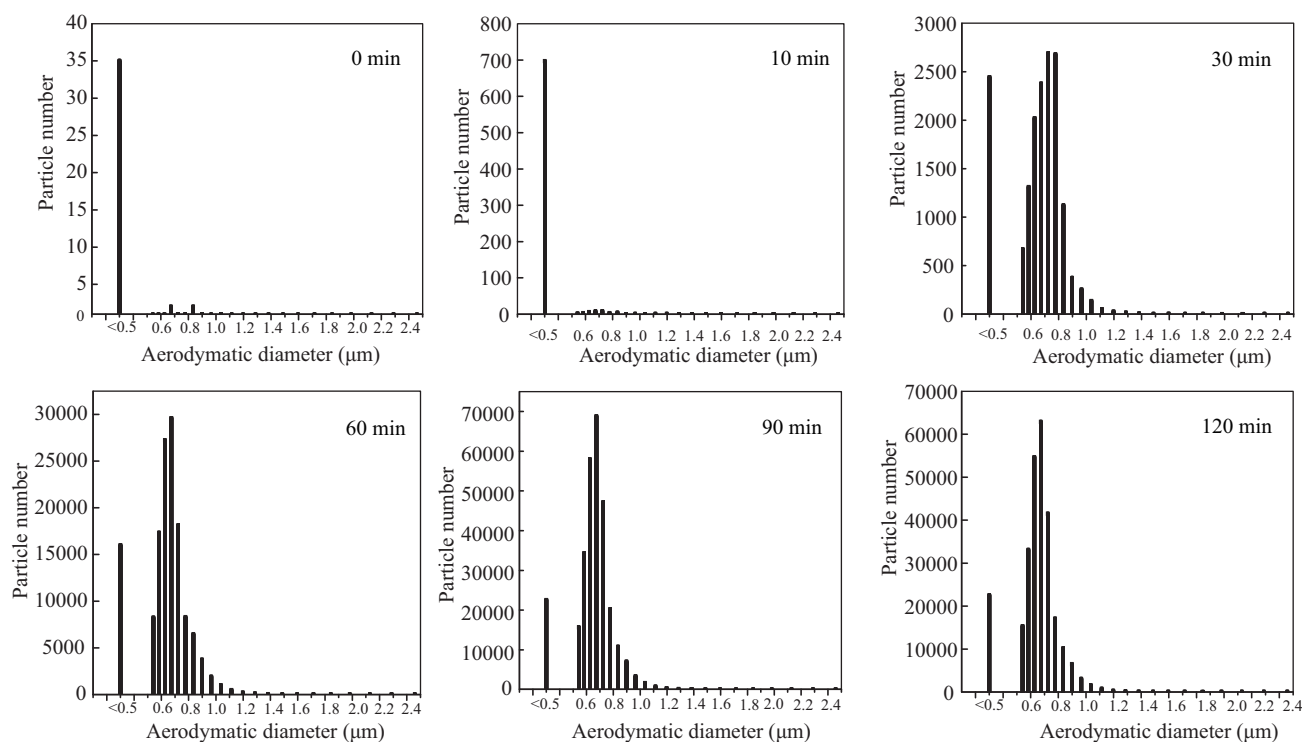
Fig. 1 Size distribution of SOA particles formed from Cl-initiated oxidation of toluene at different reaction time.

saturation concentration no aerosol will be formed. After the reaction time of 10 min, the rate of its subsequent reaction becomes quicker than before, the number of SOA particles will be increased due to that more semi-volatile organic compounds are partitioned between gas phase and particle phases. It was followed that the fine particles matter became larger through a self-nucleation or condense on the pre-exiting aerosol process. After 90 min, the total reaction system would be in short equilibrium state as soon as the formation rate of fine particles was equal to that of large particles condensed, the number density of SOA reached the concentration of 3200 particles/cm^3. However, after 120 min, the particle number of SOA then decreased with the reaction time. This is because the Cl atoms has been almost completely consumed, SOA particles shift to the larger particle size with the reaction time, and as the result of turbulent, Brownian diffusion, gravitational sedimentation, SOA particles deposition onto the wall of the smog chamber (Bowman et al., 1997).

The experimental results were compared with the results of toluene OH-initiated oxidation experiment (Hao et al., 2005), which showed that the number of SOA particles reached 2300 particles/cm^3 after 130 min photooxidation. Compared with OH radicals, Cl atoms can accelerate the growth rate of SOA and shorten the time to equilibrium state. It seemed that Cl atoms have greater contribution to the formation of SOA than that of OH radicals. And the SOA particles created by Cl-initiated oxidation of toluene are predominant in the form of fine particles, which

have diameter (0.3–1.2 μm), being less than 2.5 μm (i.e., PM2.5). Scientific research have proved that these fine particles can easily deposit in the lung, and do great harm to human health (Schwartz et al., 1996).

2.2 Laser desorption/ionization (LDI) mass spectra of toluene SOA particles

According to the design principles on the measuring system of particle diameter, timing circuit, and laser desorption/ionization setup of ALTOFMS, its time of flight mass spectroscopy is only obtained from those particles of secondary organic aerosol, whose diameter has been measured. The positive laser desorption/ionization mass spectra of SOA particles are shown in Fig. 3. It is seen that each piece of mass spectrum corresponds to an aerosol particle, and the diameter and chemical composition might be different from each other.

As we known, the intensity of the mass peak is a good parameter for quantitative analysis the products of SOA. However, our experiments have been obtained 1876 pieces of mass spectra; it is very difficult to analyze the intensity of the mass peak for each piece of mass peak. In order to obtain product information of SOA, we had to temporarily focus the intensity of mass peaks, but by statistical mass peak frequency to qualitative analysis of SOA products. Therefore, a software compiled in Visual C^{++} was developed by our laboratory. Using this software, we can get the total number (N_0) of mass spectra of the experiment of toluene. Also, the number (n) of mass
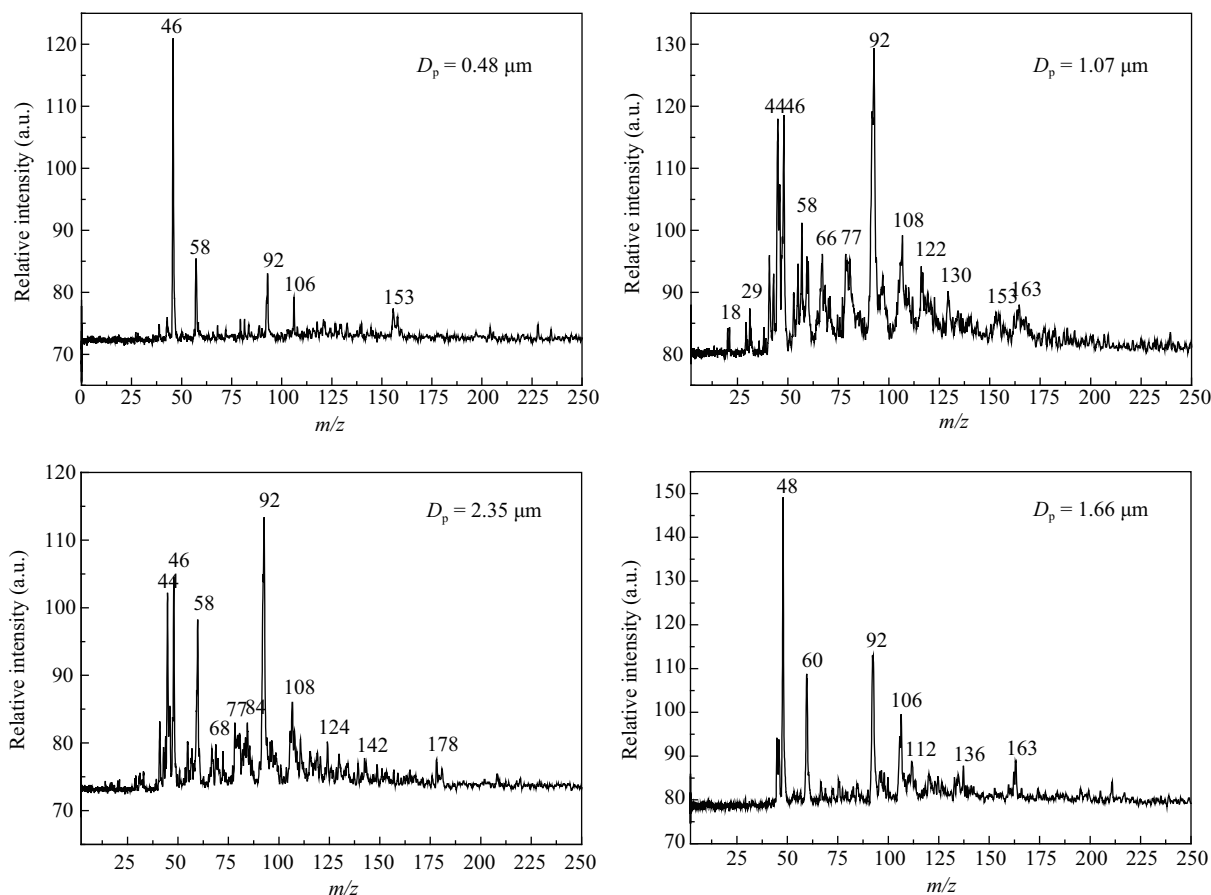
Fig. 3   Laser desorption/ionization time-of-flight mass spectra and size of 4 individual toluene SOA particles after 1 hour photooxidation.

spectra including a defined ratio of m/z can be picked out from that total number (N_0) of mass spectra. The ratio of n to N_0 is defined as: η ($\eta = n/N_0$). For example, $N_0 = 1876$, and $n = 600$ for mass spectra including $m/z = 106$, $\eta = 32\%$. Table 1 lists η of main mass spectra peaks, possible fragment ions, and the molecular structures of speculated products for Cl-initiated oxidation of toluene, while m/z was 66, 112, 130, 136, 142, 163 and 178, representing some unidentified compounds.

These oxidation products can be divided into aromatic ring retaining product (benzaldehyde, benzyl alcohol, benzoic acid, benzyl hydroperoxide, benzyl methyl nitrate), nonaromatic ring reserved product (benzoquinone) and ring-opened carbonyl product (glyoxal). As shown in Fig. 4, following the initial H-atom abstraction process by Cl atoms, the benzyl peroxy radicals formed can undergo selfreaction to form benzyl alcohol and benzaldehyde, or react with HO_2 to form benzyl hydroperoxide (Wang et al., 2005). In the presence of NO, benzyl peroxy radicals

may react with NO to form benzyl methyl nitrate, or to form the corresponding alkoxy radical, oxygen can abstract a hydrogen atom from the alkoxy radical to form benzaldehyde, which can further reaction to form benzoic acid and benzoquinone and to propagate the radical chain reaction (Cai et al., 2008). Figure 4 also outlines this suggested mechanism leading to benzoquinone.

In the presence of NO, ALTOFMS analyses showed, in addition to the products mentioned above, product with molecular weight of 58. This product is attributed to glyoxal, by analogy to product observed by Jang and Kamens (2001). in the OH radical-initiated reaction with toluene. As shown in Fig. 4, in the presence of NO, HO_2 radicals formed from the reactions of $C_6H_5CH_2O$ radicals with O_2 react with NO to form OH radicals, which then react with toluene, leading to formation of the ring-opened dicarbonyls glyoxal (Jang and Kamens, 2001; Wang et al., 2005).

Table 1   Molecular structure of speculated SOA products from Cl-initiated oxidation of toluene

Observed M^+ ion (m/z)	Ratio $\eta^{[a]}$	Possible fragment ions (m/z)	Products	Structure	Ref. & Comment
58	18%	29 (HCO^+)	Glyoxal	$H(O)C\text{-}C(O)H$	Tentatively identified
106	32%	29 (HCO^+), 77($C_6H_5^+$)	Benzaldehyde	C_6H_5CHO	Wang et al., 1997; Cai et al., 2008
108	21%	18 (H_2O^+), 77($C_6H_5^+$)	Benzyl alcohol	$C_6H_5CH_2OH$	Wang et al., 1997; Cai et al., 2008
		82 ($C_4H_2O_2^+$)	Benzoquinone	$C_6H_4O_2$	Cai et al., 2008
122	16%	44 (COO^+), 77($C_6H_5^+$)	Benzoic acid	C_6H_5COOH	Wang et al., 1997; Cai et al., 2008
124	13%	18 (H_2O^+), 77($C_6H_5^+$)	Benzyl hydroperoxide	$C_6H_5CH_2OOH$	Cai et al., 2008
153	11%	46(NO_2^+), 77($C_6H_5^+$)	Benzyl methyl nitrate	$C_6H_5CH_2ONO_2$	Tentatively identified

[a] Ratio η is defined as the number of mass spectra to the total number of mass spectra.
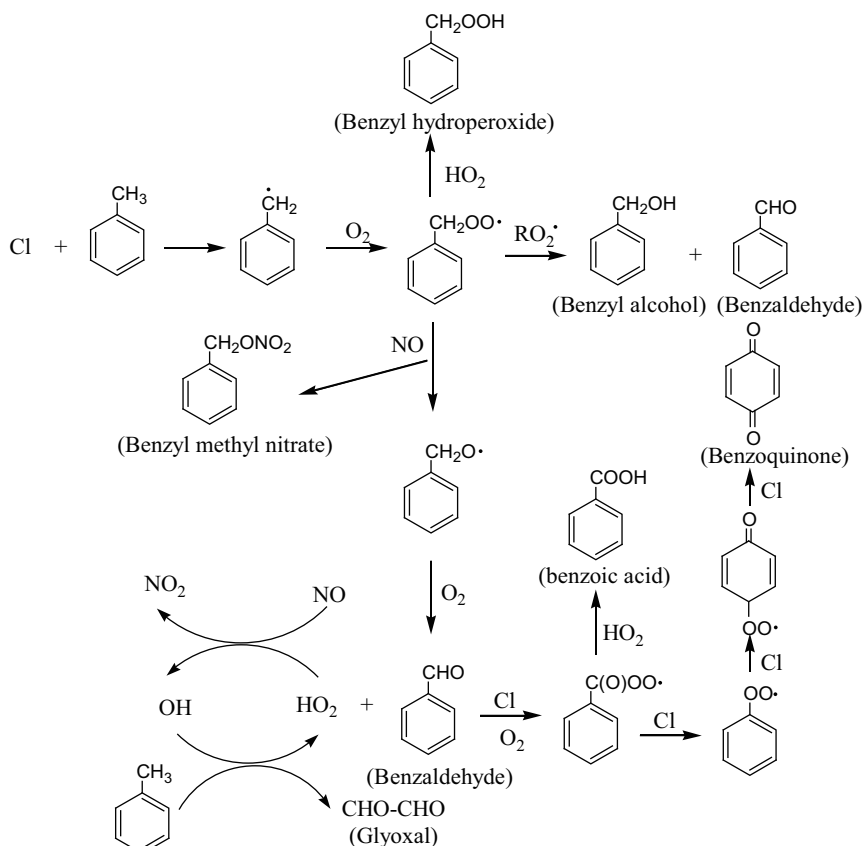
Fig. 4   Proposed reaction mechanism for Cl-initiated oxidation of toluene.

3 Conclusions

A laboratory study was carried out to investigate the Cl-initiated oxidation of toluene in a smog chamber. The aerodynamic particle size spectrometer and aerosol time of flight mass spectrometer were employed to simultaneously detect the size distribution and chemical composition of SOA particles, respectively. SOA particles created by Cl-initiated oxidation of toluene is predominantly in the form of PM 2.5 fine particles, and glyoxal, benzaldehyde, benzyl alcohol, benzoquinone, benzoic acid, benzyl hydroperoxide and benzyl methyl nitrate are major products components in the SOA. This will provide new information on the mechanism of the Cl-initiated photooxidation of toluene. In this work, we did not investigate the products of SOA quantitatively, which need to be addressed using methods such as GC-MS in further experimental investigations.

References

Ariya P A, Niki H, Harris G W, Anlauf K G, Worthy D E J, 1999. Polar sunrise experiment 1995: hydrocarbon measurements and tropospheric Cl and Br-atoms chemistry. *Atmospheric Environment*, 33(6): 931–938.

Atkinson R, Arey J, 2003. Atmospheric degradation of volatile organic compounds. *Chemical Reviews*, 103(12): 4605–4638.

Atkinson R, Aschmann S M, 1985. Kinetics of the gas phase reaction of Cl atoms with a series of organics at 296 ± 2 K and atmospheric pressure. *International Journal of Chemical Kinetics*, 17(1): 33–41.

Bowman F M, Odum J R, Seinfeld J H, Pandis S N, 1997. Mathematical model for gas-particle partitioning of secondary organic aerosols. *Atmospheric Environment*, 31(23): 3921–3931.

Cai X Y, Ziemba L D, Griffin R J, 2008. Secondary aerosol formation from the oxidation of toluene by chlorine atoms. *Atmospheric Environment*, 42(32): 7348–7359.

Fantechi G, Jensen N R, Saastad O, Hjorth J, Peeters J, 1998. Reactions of Cl atoms with selected VOCs: kinetics, products and mechanisms. *Journal of Atmospheric Chemistry*, 31(3): 247–267.

Hao L Q, Wang Z Y, Huang M Q, Fang L, Zhang W J, 2007. Effects of seed aerosols on the growth of secondary organic aerosols from the photooxidation of toluene. *Journal of Environmental Sciences*, 19(6): 704–708.

Hao L Q, Wang Z Y, Huang M Q, Pei S X, Yang Y, Zhang W J, 2005. Size distribution of the secondary organic aerosol particles from the photooxidation of toluene. *Journal of Environmental Sciences*, 17(16): 912–916.

Huang M Q, Zhang W J, Hao L Q, Wang Z Y, Fang L, Kong R H et al., 2010. Experimental study of photooxidation products of ethylbenzene. *Journal of Environmental Sciences*, 22(10): 1570–1575.

Jang M S, Kamens R M, 2001. Characterization of secondary aerosol from the photooxidation of toluene in the presence of NO$_x$ and 1-propene. *Environmental Science and Technology*, 35(18): 3626–3639.

Karlsson R S, SzenteJ J, Ball J C, Maricq M M, 2001. Homogeneous aerosol formation by the chlorine atom initiated oxidation of toluene. *Journal of Physical Chemistry A*, 105(1): 82–96.

Kercher J P, Riedel T P, Thorton J A, 2009. Chlorine activation by N$_2$O$_5$: simultaneous, in situ detection of ClNO$_2$ and N$_2$O$_5$ by chemical ionization mass spectrometry. *Atmospheric Measurement Techniques*, 2(1): 193–204

Notario A, Mellouki A, Le Bars G, 2000. Rate constants for the gas-phase reactions of chlorine atoms with a series of ketones. *International Journal of Chemical Kinetics*, 32(1): 62–66.

Odum J R, Hoffman T, Bowman F, Collins D, Flagan R C, Seinfeld J H, 1996. Gas/particle partitioning and secondary organic aerosol yields. *Environmental Science and Technology*, 30(8): 2580–2585.

Odum J R, Jungkamp T P W, Griffin R J, Flagan R C, Seinfeld J H, 1997. The atmospheric aerosol-forming potential of whole gasoline vapor. *Science*, 276(5309): 96–99.

Oum K W, Lakin M J, Dehaan D O, Brauers T, Finlayson-Pitts B J, 1998. Formation of molecular chlorine from the photolysis of ozone and aqueous sea-salt particles. *Science*, 279(5347): 74–76.

Ramacher B, Rudolph J, Koppmann R, 1997. Hydrocarbon measurements in the spring arctic troposphere during the ARCTOC 95 campaign. *Tellus Series B*, 49B(5): 466–485.

Shi J C, Bernhard M J, 1997. Kinetic studies of Cl-atom reactions with selected aromatic compounds using the photochemical reactor-FTIR spectroscopy technique. *International Journal of Chemical Kinetics*, 29(5): 349–358.

Spicer C W, Chapman E G, Finlayson-Pitts B J, Plastridge R A, Hubbe J M, Fast J D et al., 1998. Unexpectedly high concentrations of molecular chlorine in coastal air. *Nature*, 394(6691): 353–356.

Thiault G, Mellouki A, Le Bras G, 2002. Kinetics of gas phase reactions of OH and Cl with aromatic aldehydes. *Physical Chemistry Chemical Physics*, 4(11): 2194–2199.

Wang L, Arey J, Atkinson R, 2005. Reactions of chlorine atoms with a series of aromatic hydrocarbons. *Environmental Science and Technology*, 39(14): 5302–5310.

Wingenter O W, Blake D R, Blake N J, Sive B C, Rowland F S, Atlas E et al., 1999. Tropospheric hydroxyl and atomic chlorine concentrations, and mixing timescales determined from hydrocarbon and halocarbon measurements made over the Southern Ocean. *Journal of Geophysical Research*, 104(D17): 21819–21828.